

16-Row CT-Coronary Angiography. Influence of Reconstruction Technique and Heart Rate upon Diagnostic Accuracy

For submission in Circulation, clinical investigation

Background: To develop an optimal image reconstruction strategy for multidetector-row CT coronary angiography (MD-CTA) and to investigate its accuracy at different heart rates.

Methods and Results: 70 patients consecutively underwent 16-row MD-CTA, 50 patients additionally had an invasive coronary angiography. Image reconstruction was performed both antegrade-proportional and antegrade-absolute in relation to the previous R-peak. Using a four-step Likert grading scale, optimal antegrade-proportional reconstruction intervals were derived from data sets differing by 5% each and optimal antegrade-absolute reconstruction intervals from data sets, differing by 10 ms each. Cluster, discrimination and regression analysis were applied to identify optimal reconstruction intervals for heart rates (HR) between 45 and 103 bpm. Antegrade-absolute image reconstruction led to significantly better image quality than antegrade-proportional image reconstruction ($p < 10^{-6}$). Best results were observed for LCA and LCX and for low HR. Cluster analysis showed a significant correlation between the amount of HR and the R-R position of the reconstruction interval, revealing optimal image quality almost exclusively for either end-diastolic (low HR) or end-systolic (elevated HR) reconstructions (cut-off HR: 64.5-67.5 bpm). Stenoses $>75\%$ were identified with 86.7 % sensitivity and 97.6% specificity by using antegrade-absolute reconstruction and with 83.3 % sensitivity and 97.9% specificity by using antegrade-proportional reconstruction, showing no significant difference ($p=0.98$).

Conclusion: Image quality in multidetector-row CT coronary angiography critically depends on both correct positioning of the reconstruction interval and choice of a suited reconstruction algorithm. Combined adequately, sufficient image evaluation is feasible even in the presence of elevated heart rates.

Condensed abstract:

70 patients underwent 16-row CT coronary angiography. Image reconstruction was performed in steps of 5%, 10 ms respectively, antegrade-proportional and antegrade-absolute in relation to the previous R-peak. 30 patients additionally had coronary angiography. Antegrade-absolute reconstruction led to significantly better image quality ($p < 10^{-6}$). Best results were observed for LCA and LCX and for low HR. A significant correlation between the amount of HR and the R-R position of the reconstruction interval was observed, revealing optimal image quality only for end-diastolic (low HR) or end-systolic (elevated HR) reconstructions (cut-off HR: 64.5-67.5 bpm). Stenoses $>75\%$ were identified with 86.7 % sensitivity and 97.6% specificity by antegrade-absolute reconstruction showing no significant difference to antegrade-proportional reconstruction ($p=0.98$).

Key Words: Multidetector-row Computed Tomography – Cardiac CT – Image Reconstruction – CT Coronary Angiography

Introduction

The recent introduction of 16-row CT technology is commonly regarded as a further step towards non-invasive CT cardiac imaging. Particularly the combination of subsecond rotation and submillimeter collimation¹ resolved the long-lasting trade-off between scan volume and slice thickness, now rendering possible acquisition of large scan volumes in submillimeter slice thickness. However in cardiac imaging, image quality unfortunately is less determined by spatial than by temporal resolution. By using conventional image reconstruction algorithms (i.e. 180° interpolation) temporal resolution at present ranges between 250 and 187 ms depending on which scanner is used^{1,2}. For motion artifact free image quality consequently the average R-R cycle duration must allow for at least 187-250 ms of cardiac akinesia. At low heart rates this is easily achieved by placing the reconstruction interval somewhere in the - relatively long lasting and rather tranquil - end-diastole (diastase). However at elevated heart rates, this phase distinctly diminishes until it finally completely disappears^{3,4}.

All manufacturers try to compensate for this physiological limitation by applying different – yet still comparable - multi-phase image reconstruction protocols. The similarity of these protocols lies in the combination of data derived from several adjacent R-R intervals for the reconstruction of each transversal CT image^{1,2}. Depending on the manufacturer these cardiac-CT specific reconstruction algorithms are typically employed at heart rates >65-75 bpm. By this means temporal resolution (i.e. image acquisition time) can be reduced to values as low as 80 ms². However, at higher heart rates this is still insufficient and thus may be one reason why diagnostic accuracy of MDCT still lags behind that of invasive coronary angiography^{5,6}. In addition, due to multi-segment image reconstruction, cardiac CT scanners often

express a rather confusing behaviour in terms of temporal resolution. The Somatom Sensation 16 (Siemens Inc., Forchheim, Germany) for example achieves optimal temporal resolutions only twice, at heart rates of approximately 80 bpm and 115 bpm (Figure 1).

The aim of this study, therefore, was to evaluate image quality of CT coronary angiography at different heart rates, to determine the prevailing optimal reconstruction intervals and to correlate the results with those obtained from coronary angiograms.

Methods

Patients

In a prospective randomized study seventy consecutive patients (49 males and 21 females) underwent cardiac multidetector-row CT (MDCT). Of these, fifty patients (33 males and 17 females) additionally had invasive coronary angiography (CA). The mean time between both examinations amounted to 13 days (range 3 to 19 days). The study was approved by our ethics review board and all patients had previously signed informed consent. The patients' average age was 59.1 years (range 29 to 65 years), their mean heart rate amounted to 70.7 beats per minute (bpm) (range 45 to 121 bpm). Patients with absolute tachyarrhythmia or irregular heart rates – i.e. >15 bpm difference between minimum and maximum value – were not included into the study.

Image acquisition

MDCT examinations were performed on a 16-row spiral CT (Sensation 16, Siemens Inc., Forchheim, Germany) and all patients were scanned at their original heart. Scanning parameters were 120 kV voltage and 400 mAs tube current, 420 ms rotation time, 16 x 0.75 mm collimation, and 2.8 mm table feed per rotation. Each patient received 90 ml of a non-ionic contrast medium (Ultravist® 370 mgI/ml; Schering Inc., Berlin, Germany) infused through an 18G intravenous antecubital catheter. A tri-phase protocol for contrast medium application was applied by using bolus triggering technique: 30 ml CM @ 4.5 ml/s, 60 ml CM @ 2.5 ml/s and 30 ml sodium chloride @ 2.5 ml⁷.

Image reconstruction

Image reconstruction in all patients was performed using retrospective ECG gating, a technique that allowed continuous image reconstruction from volume data sets during any phase of the cardiac cycle. Reconstruction parameters were 220 mm FOV, kernel B35 (a medium soft-tissue kernel), 1.0 mm effective slice thickness and 0.5 mm increment. Adaptive Cardiac Volume (ACV®) technique, which is standardised provided with the Sensation 16 cardiac software package, served as reconstruction algorithm. Up to heart rates ≤ 72 bpm ACV allows for single-segmental reconstruction, at heart rates > 72 bpm for two-segment reconstruction of each 1.25 mm slice⁸. While temporal resolution for single-segment-reconstruction constantly was 210 ms, for two-segment reconstruction it ranged between 210 and 105 ms subject to the heart rate⁸. This rather confusing pattern is particularly specific for Siemens CT's but may be observed in a similar way also in other manufacturer's scanners (Figure 1).

Determination of image quality and optimal reconstruction intervals

In order to determine reconstruction intervals that allowed for optimal image quality at different heart rates, in all patients image reconstruction was performed antegrade-proportional and antegrade-absolute in relation to the previous R-peak .

Optimal antegrade-proportional reconstruction intervals were chosen from data sets that had been reconstructed twenty-fold in steps of 5%. The first reconstruction was done at 0%, the last reconstruction at 95% of the R-R interval.

Optimal antegrade-absolute reconstruction intervals were chosen from data sets that equally were reconstructed twenty-fold within the R-R interval. Hence all data sets initially were reconstructed tenfold in equidistant steps (calculation formula: $60000 \text{ ms} / \text{HR (bpm)} / 10$). Subsequently the step showing the least motion artifacts was

determined (details see below) and image reconstruction was repeated each fivefold before and behind this value (this time in steps of each 10 ms).

After previous blinding of both antegrade-proportional and antegrade-absolute data sets, assessment with regard to optimal image quality was performed by two independent observers. Proximal, medial and distal sections of RCA, LCA, and LCX were examined separately. Proximal included segments 1 (RCA), 5 and 6 (LCA) and 11 (LCX), medial segments 2 and 3 (RCA), 7 (LCA) and 13 (LCX), distal segments 4 (RCA), 8 (LCA), 15 (LCX). Image evaluation was done exclusively on transverse scans since exact assignment of the prevailing heart rate to the current slice position was possible only with this approach – both are specified in the image comment of the transverse scan. All evaluations were performed on a separate workstation (Leonardo ®, Siemens Inc., Forchheim, Germany) with 512 x 512 matrix size. The criterion to be analyzed was the in-plane motion of the prevailing vascular section. A four-step Likert grading scale allowed objective classification into 4 groups: excellent (1), good (2), moderate (3) and poor (4) image quality. Excellent quality was attributed to vessels appearing as a clear circular/oval area surrounded by low-attenuation fat tissue and showing no motion artifacts. The same applied to calcified atherosclerotic plaques in this group. Good quality was attributed to the presence of discrete blurring of the vessels' or calcified plaques' margin, and slight motion artifacts, seen as a discrete tail or streak emitting shadow on at least one level. Moderate image quality showed noticeably blurred vessel- / plaque margins and distinctly broader motion artifacts extending less than 5 mm from the vessels' center. Poor image quality was defined by inadequate delineation between vessel and surrounding tissue as well as by streak artifacts extending at least 5 mm from the center of the vessel (Figure 2).

Comparison to coronary angiograms

Effective clinical benefit of optimal image reconstruction could be evaluated in 50 of the 70 patients who additionally underwent invasive coronary angiography. Analysis of the CT scans was performed by the same two independent observers as above in consensus, and on data sets which had previously been blinded. Multiplanar reformations, maximum intensity projections and transverse scans were assessed. All MDCT findings were compared to corresponding coronary angiograms, which had been performed in different technical systems using the Judkin's technique. At least four views of the left and two views of the right coronary artery system were analyzed by an experienced observer, who was trained in this technique and who had no knowledge of the CT results in order to avoid recall bias.

Criteria to be analyzed were the number of visible coronary artery segments and the prevailing degree of stenosis. Visibility, in this context, determined if a coronary artery segment could be properly evaluated (i.e. was visible) or not.

The degree of stenosis was assessed following the classifications of the American Heart Association (AHA), which subdivide the coronary artery territory into 15 segments and distinguish between 6 different degrees of atherosclerosis⁹: (I) irregular wall outline with < 25% stenosis; (II) slight stenosis (25-50%); (III) moderate stenosis (51-74%); (IV) hemodynamically relevant stenosis (75%-89%); subtotal stenosis (90-99%) and (V) vascular occlusion (100%).

The degree of stenosis on MDCT scans was ascertained on multiplanar reformations, performed strictly orthogonally through the vessel's course, by using a semi-automated distance measuring tool (Vessel Navigator®, Siemens Inc., Erlangen, Germany). On angiograms a stenosis-grading tool with automatic distance and scale calibration was applied for the measurements (Axiom-Artis, VA21C, Siemens Inc, Forchheim, Germany).

Statistical Analysis

Statistical analysis was performed by using BiAS, version 7.0 (Epsilon Publishers, Mannheim, Germany).

The agreement between the investigators for the evaluation of image quality (1-4) was calculated by means of the κ statistic.

Differences in image quality achieved with either antegrade-proportional or antegrade-absolute reconstruction technique were tested for significance by using the Wilcoxon matched pair test.

To visualize the spreading of data and to identify possible clusters for both reconstruction techniques, McQueen-Rubin cluster analysis was performed. Evaluation was done separately for proximal, medial and distal sections of RCA, LCA and LCX. Calculation variables were the heart rate (bpm) and the optimal image quality (grade 1-4) obtained at that heart rate.

Univariate two-population distribution-free discrimination analysis was applied to identify the cut-off heart rates between the prevailing clusters.

Each cluster underwent Pearson regression analysis. In case of significant results ($p < 0.05$) mean optimal reconstruction intervals were calculated based on the prevailing regression equation.

In the 30 patients who underwent both MD-CTA and invasive coronary angiography, the number of coronary segments visible on MDCT scans was determined in proportion to the number of segments visualized on coronary angiograms.

Correlation between CA and MD-CTA in the detection and grading of coronary atherosclerosis was evaluated by using the Spearman's correlation. The Bowker's test was applied to check the symmetry of the data distribution and to evaluate possible under-/overestimation through MD-CTA.

Any relationship between heart rate and prevailing correlation coefficient was investigated by calculation of separate total correlation coefficients for each of the 30 patients and subsequent correlation with the prevailing average heart rate. Statistical methods were the Spearman correlation and the Fisher exact test.

Sensitivity and specificity as well as positive and negative predictive value of MD-CTA in the detection of hemodynamically relevant stenoses (HRS) was determined on cross tables. HRS defined stenosis >75% on the angiogram⁹, i.e. AHA groups IV, V and VI. Any differences in the results of absolute and proportional image reconstruction were tested for significance by using Chi² contingency tables.

Results

Optimal image reconstruction intervals

In total 2,800 reconstructions were performed. The agreement between observers in the definition of optimal reconstruction intervals amounted to 0.96 (95% CI: 0.963; 0.972) for antegrade-proportional image reconstruction and to 0.87 (95% CI: 0.859; 0.895) for antegrade-absolute image reconstruction. Since this was regarded as an excellent, very good respectively, agreement all subsequent calculations were performed based on matched data of both investigators.

Image quality was significantly better ($p < 10^{-6}$) for antegrade-absolute than for antegrade-proportional reconstructions, differing by 0.25 grading points (95% CI: 2.00; 3.00) on average (Tables 1a-c). Both techniques led to better results for LCA than for RCA or LCX., showing only minor differences between proximal, medial and distal sections (Tables 1a-c). Irrespective of the reconstruction technique or vessel section, better image quality was achieved at lower than at elevated heart rates (Tables 1a-c). By using antegrade-absolute image reconstruction persistent good image quality (i.e. grading ≤ 2.5) was obtained for heart rates up to 90 bpm (Figure 3), by using antegrade-proportional image reconstruction for heart rates up to 70 bpm.

Cluster analysis showed a significant correlation between the R-R position of reconstruction interval and the amount of heart rate. Optimal image quality was almost exclusively observed for either end-diastolic (lower heart rates) or end-systolic (elevated heart rates) reconstructions. The cut-off heart rates for end-systolic and end-diastolic clusters ranged between 65.0 bpm and 68.5 bpm (Table 2, 3).

End-diastolic clusters for antegrade-proportional image reconstruction (ap) ranged from 40% to 75% with cluster centers from 59.4% to 62.2% (Table 2), end-systolic

clusters from 10% to 35% with centers from 26.3% to 28.3% (Table 2) respectively. For antegrade-absolute image reconstruction (aa) end-diastolic clusters ranged from 450 ms to 880 ms with cluster centers from 568 ms to 621 ms (Table 3) and end-systolic clusters from 80 ms to 350 ms with centers from 193 ms to 212 ms (Table 3).

The Pearson regression showed significant results only for clusters obtained from antegrade-absolute image reconstruction (Table 2, 3), thus allowing calculation of optimal reconstruction intervals based on the regression equations only for this reconstruction technique. Optimal intervals for antegrade-proportional image reconstruction were approximated from the prevailing cluster centres (Table 2).

Correlation between CTA and coronary angiograms

The 50 patients who underwent both MD-CTA and invasive coronary angiography had heart rates 52-105 bpm. 436 coronary artery segments were visible on angiograms, of which 384 (87.9%) were visualized by using antegrade-proportional image reconstruction and 388 (88.9%) by using antegrade-absolute image reconstruction. Each 14 segments were missed due to a diameter <1.5 mm and 3 due to heavy calcifications by both reconstruction techniques, the remaining 35 (antegrade-proportional image reconstruction), 31 (antegrade-absolute image reconstruction) respectively, segments could not be visualized due to marked motion artifacts.

In the detection and grading of atherosclerosis (AHA I-VI) total correlation coefficients were 0.52 (range: 0.21-0.79 / $p < 0.01$) for antegrade-proportional and 0.57 (range: 0.18-0.79 / $p < 0.01$) for antegrade-absolute image reconstruction (Table 4). The Bowker's test showed a rather symmetrical distribution of the data for both antegrade-proportional ($p = 0.68$) and antegrade-absolute image reconstruction

($p=0.71$). Antegrade-proportional image reconstruction underestimated and overestimated each 33.3 % (48/143) of all stenoses, antegrade-absolute image reconstruction 31.9% (46/144) and 17.4 % (25/144) of all stenoses. No correlation was observed between the heart rate and the prevailing coefficient of correlation (Figure 4): antegrade-proportional image reconstruction ($r = -0.002 / p>0.20$); antegrade-absolute image reconstruction ($r = -0.172 / p>0.20$).

Hemodynamically relevant ($>75\%$) stenoses were identified by MD-CTA with 83.3 % sensitivity (25/30; 95% CI: 65.3%; 94.4%) and 97.9% specificity (411/420; 95% CI: 96.0%; 99.1%) by using absolute-proportional image reconstruction. PPV amounted to 73.5% (25/34; 95% CI: 55.7%; 87.1%), NPV to 98.8% (411/416; 95% CI: 97.2%; 99.6%). All 5 HRS overlooked were located in diagonal branches of the LCA that either showed marked motion artifacts due to heart rates >90 bpm ($n=2$) or were <1.5 mm in diameter ($n=3$). By using antegrade-absolute image reconstruction sensitivity amounted to 86.7 % (26/30; 95% CI: 69.3%; 96.2%), specificity to 97.6% (410/420; 95% CI: 95.7%; 98.9%), PPV to 72.2% (26/36; 95% CI: 54.8%; 85.8%) and NPV to 99.0% (410/414; 95% CI: 97.5%; 99.7%). One HRS was missed due to marked motion artifacts, the remaining three due to vascular diameters <1.5 mm. The results obtained with both reconstruction techniques were not significantly different ($p=0.98$).

Discussion

Our findings correspond very well with the observations made by Mao et al. on Electron Beam Computed Tomography (EBCT) ¹⁰, who calculated optimal trigger times for 200 ms and 250 ms scans and found 60-65% of R-R ideal for heart rates \leq 60 bpm and 27-39% for heart rates $>$ 60 bpm. Similar to our results triggering based on absolute times resulted in the fewest motion artifacts and thus in better image quality. Moreover, the last 50 ms of the end-systole, i.e. the last 30-50 ms before the end of the t-wave, proved to be an optimal trigger point for 100- ms scan times, showing virtually no motion artifacts across all heart rates. It seems that the end of the t-wave is identical to 30-50% of the R-R interval in which, according to others, coronary arteries, in general, show the slowest motion ^{11,12}.

These findings correspond well with cardiac physiology. The systole consists of two main periods: the isometric contraction phase following the auricular systole, and the ejection phase which can be subdivided into an early phase of maximum ejection and a later phase of reduced or absent ejection ^{3,13}. The latter describes the time between steep pressure increase in the aorta and the beginning of the incisura, in early studies by Patterson, Piper and Starling “a condition in which the ventricles remain contracted without expelling any blood” ¹⁴.

The reduced ejection phase is immediately followed by two akin motionless phases, the proto-diastole and the diastolic phase of isovolumetric relaxation ^{4,15} (Fig. 8). The latter designates the interval between closure of the semilunar valves and opening of the atrio-ventricular valves ^{3,16}, whereas the proto-diastole represents the time between the end of ventricular contraction and valve closure ⁴. Combination of these three consecutive phases thus theoretically gives rise to an almost inert

reconstruction window of approximately 202 ms for the left coronary artery system and approximately 179 ms for the right coronary artery system^{3,4,15,16}.

However, whereas for EBCT excellent results were obtained across all heart rates¹⁰ within this interval, for MDCT this was only true for elevated heart rates. At lower heart rates markedly better image quality was derived from end-diastolic reconstructions. It seems that two antidromic factors may be relevant for this : a decrease in the duration of the end-diastolic reconstruction interval^{4,16} combined with superior temporal resolution at increasing heart rates^{1,17}.

While the latter is effected by multi-segment image reconstruction (Figure 1), the former is caused by a continuous diminishing of the diastase at increasing heart rates. This phase, squeezed between the very rough phase of rapid ventricular filling^{3,4,13,18} and the akin rough auricular systole, represents the only diastolic time range which is both long and calm enough for sufficient image reconstruction. However, Henderson et al. pointed out that “the stage of diastasis is non-existent whenever the total period of diastole does not exceed the time taken for rapid inflow”³, i.e. at the latest if the heart rate exceeds ~95 bpm^{3,4,18}.

Thus, from a physiological point of view sufficient image reconstruction within the diastase may be feasible only at lower heart rates, whereas at higher heart rates an end-systolic image reconstruction appears more favourable. Cut-off values for the 16-row scanner in this study ranged around 67 bpm.

The significant better image quality of antegrade-absolute image reconstruction as compared to antegrade-proportional image reconstruction may also be due to these physiological prerequisites. Antegrade-proportional image reconstruction is performed relative to the total R-R distance and thus relies on the duration of both the systole and the diastole. Any changes in the heart rate, which preferably impact on the duration of the diastole, thus directly affect the R-R allocation of the prevailing

antegrade-proportional reconstruction interval. Antegrade-absolute image reconstruction on the other hand is performed at a fixed time after the previous R-peak and therefore mainly relies on the duration of the systole, which is not as strongly influenced by alterations in the heart rate. The R-R allocation of antegrade-absolute reconstruction intervals thus will be less influenced by heart rate changes. This is particularly important at elevated heart rates where the available systolic R-R interval allowing for relatively motion artefact free image reconstruction is only short and exact R-R allocation of the reconstruction interval thus is indispensable¹⁰. However the only discrete differences of both reconstruction techniques in the detection of hemodynamically relevant stenoses indicate that the clinical impact in fact may be only marginally.

A careful interpretation of our findings could also explain the alleged contradiction to other studies, who described sufficient image quality at 40-50% of R-R for the right and at 50-70% of R-R for the left coronary system. However, those reconstruction intervals were determined nearly exclusively for average heart rates between 63-72 bpm^{12,19-22}, and thus for a range where the scanner's temporal resolution still suffices for end-diastolic image reconstruction.

Unfortunately the present study is limited in several ways. First of all the small number of patients included unfortunately limits the informational value of our results. The authors tried to make allowance for this by including confidence intervals for all relevant values. Their large variability nevertheless indicates that accuracy for sensitivity, specificity NPV and PPV is rather low. Second, a possible effect of z-axis motion, as described by others, has not been taken into account¹⁰. Any minimal undesired change in the z-axis could theoretically induce imaging misregistration. However, according to others the z-axis motion is proportional to that of the x-y plane and thus possible adverse influences by this effect were regarded as

negligible²³. Third, any possible negative effect of using multi-segment reconstruction has also been disregarded. By combining data from at least two different R-R cycles for reconstruction of each single image¹⁷, the algorithm itself may induce artificial blurring of the images²⁴. Further studies in this direction are strongly encouraged. Finally, no information is given regarding the radiation dose, a particularly important point as multi-segment image reconstruction requires a reduced table feed per rotation and consequently higher individual doses than single-segment reconstruction²⁵ or coronary angiograms²⁶. Any analysis in this respect unfortunately was beyond the range of this study and multi-segment reconstruction in addition presently is the only viable reconstruction technique for tachycardic patients^{1,2}. However, these observations certainly demand for further technical developments and a thorough indication for each cardiac-CT²⁷.

In conclusion, our results indicate that in 16-row cardiac CT image quality - and thus diagnostic accuracy – very much depends on the choice of an appropriate reconstruction interval. They further suggest a clear relationship between the R-R position of that interval and the heart rate. Apparently optimal image quality is observed at elevated heart rates in the end-systole/early-diastole and at lower heart rates in the end-diastole. Antegrade-absolute image reconstruction proved to result in superior image quality and thus in better clinical correlation. Scanning at low heart rates appears preferable since temporal resolution still is insufficient for patients with tachycardia. Betablocker medication prior to the examination may be regarded as a useful approach to induce bradycardia. Due to similar image acquisition and reconstruction techniques^{1,2}, the underlying physiological rationale should be similar also for any other available cardiac scanner.

References

1. Flohr TG, Schoepf UJ, Kuettner A, Halliburton S, Bruder H, Suess C, Schmidt B, Hofmann L, Yucel EK, Schaller S, Ohnesorge BM. Advances in cardiac imaging with 16-section CT systems. *Acad Radiol*. 2003;10:386-401.
2. Blobel J, Baartman H, Rogalla P, Mews J, Lembcke A. Spatial and Temporal Resolution with 16-Slice Computed Tomography for Cardiac Imaging. *Fortschr Roentgenstr*. 2003;175:1264-1271.
3. Wiggers CJ. Studies on the consecutive phases of the cardiac cycle. I.) The duration of the consecutive phases of the cardiac cycle and the criteria for their precise determination. *Am J Physiol*. 1921;56:415-438.
4. Luisada AA, MacCanon DM. The phases of the cardiac cycle. *Am Heart J*. 1972;83:705-11.
5. Nieman K, Cademartiri F, Lemos PA, Raaijmakers R, Pattynama PM, de Feyter PJ. Reliable noninvasive coronary angiography with fast submillimeter multislice spiral computed tomography. *Circulation*. 2002;106:2051-4.
6. Ropers D, Baum U, Pohle K, Anders K, Ulzheimer S, Ohnesorge B, Schlundt C, Bautz W, Daniel WG, Achenbach S. Detection of coronary artery stenoses with thin-slice multi-detector row spiral computed tomography and multiplanar reconstruction. *Circulation*. 2003;107:664-6.
7. Fleischmann D. High-concentration contrast media in MDCT angiography: principles and rationale. *Eur Radiol*. 2003;13 (Suppl.3):39-43.
8. Flohr T, Ohnesorge B. Heart rate adaptive optimization of spatial and temporal resolution for electrocardiogram-gated multislice spiral CT of the heart. *J Comput Assist Tomogr*. 2001;25:907-23.
9. American College of Cardiology / American heart Association. Guidelines for cardiac catheterization and cardiac catheterization laboratories. American College of Cardiology/American Heart Association Ad Hoc Task Force on Cardiac Catheterization. *J Am Coll Cardiol*. 1991;18:1149-82.
10. Mao S, Lu B, Oudiz RJ, Bakhsheshi H, Liu SC, Budoff MJ. Coronary artery motion in electron beam tomography. *J Comput Assist Tomogr*. 2000;24:253-8.
11. Lu B, Mao SS, Zhuang N, Bakhsheshi H, Yamamoto H, Takasu J, Liu SC, Budoff MJ. Coronary artery motion during the cardiac cycle and optimal ECG triggering for coronary artery imaging. *Invest Radiol*. 2001;36:250-6.
12. Achenbach S, Ropers D, Holle J, Muschiol G, Daniel WG, Moshage W. In-plane coronary arterial motion velocity: measurement with electron-beam CT. *Radiology*. 2000;216:457-63.

13. Heiss W. Systolische und diastolische Zeitmaße des Herzzyklus. In: Roskamm H, Reindell H, eds. *Herzkrankheiten. Pathophysiologie - Diagnostik - Therapie*. 3rd ed. Berlin - Heidelberg - New York: Springer; 1989:102-112.
14. Patterson SW, Piper H, Starling EH. The regulation of the heart beat. *J Physiol*. 1914;6:465-513.
15. Arevalo F, Sakamoto T. On the duration of the isovolumetric relaxation period (IVPR) in dog and man. *Am Heart J*. 1964;67:651-656.
16. Wiggers CJ. Studies on the consecutive phases of the cardiac cycle. II.) The laws governing the relative durations of ventricular systole and diastole. *Am J Physiol*. 1921;56:439-459.
17. Flohr T, Kuttner A, Bruder H, Stierstorfer K, Halliburton SS, Schaller S, Ohnesorge BM. Performance Evaluation of a Multi-Slice CT System with 16-Slice Detector and Increased Gantry Rotation Speed for Isotropic Submillimeter Imaging of the Heart. *Herz*. 2003;28:7-19.
18. Benchimol A, Dimond EG, Carson JC. The value of the apexcardiogram as a reference tracing in phonocardiography. *Am Heart J*. 1960;61:485-493.
19. Georg C, Kopp A, Schroder S, Kuttner A, Ohnesorge B, Martensen J, Clausen CD. Optimizing image reconstruction timing for the RR interval in imaging coronary arteries with multi-slice computerized tomography. *Fortschr Rontgenstr*. 2001;173:536-41.
20. Hong C, Becker CR, Huber A, Schoepf UJ, Ohnesorge B, Knez A, Bruning R, Reiser MF. ECG-gated reconstructed multi-detector row CT coronary angiography: effect of varying trigger delay on image quality. *Radiology*. 2001;220:712-7.
21. Fischbach R, Opitz C, Juergens KU, Wichter T, Flohr T, Grude M, Fallenberg EM, Allkemper T, Heindel W. Einfluss des Rekonstruktionsintervalls auf die Qualität der Koronariendarstellung mit Mehrschicht-Spiral_CT und retrospektiver EKG-Synchronisation. *Fortschr Roentgenstr*. 2001;173:54.
22. Schroeder S, Kopp AF, Kuettner A, Burgstahler C, Herdeg C, Heuschmid M, Baumbach A, Claussen CD, Karsch KR, Seipel L. Influence of heart rate on vessel visibility in noninvasive coronary angiography using new multislice computed tomography: experience in 94 patients. *Clin Imaging*. 2002;26:106-11.
23. Wang Y, Vidan E, Bergman GW. Cardiac motion of coronary arteries: variability in the rest period and implications for coronary MR angiography. *Radiology*. 1999;213:751-8.
24. Halliburton SS, Stillman AE, Flohr T, Ohnesorge B, Obuchowski N, Lieber M, Karim W, Kuzmiak SA, Kasper JM, White RD. Do segmented reconstruction algorithms for cardiac multi-slice computed tomography improve image quality? *Herz*. 2003;28:20-31.

25. McCollough CH. Patient dose in cardiac computed tomography. *Herz*. 2003;28:1-6.
26. Hunold P, Vogt FM, Sommer T, Stoesser D, Bartsch O, Barkhausen J. Radiation exposure during coronary artery CT. Preliminary comparison of the effective doses at different multi-detector row CT scanners. *In: Radiological Society of North America scientific assembly and annual meeting program. Oak Book III: Radiological Society of North America,*. 2003:308.
27. American College of Cardiology / American heart Association. Expert Consensus Document on Electron-Beam Computed Tomography for the Diagnosis and Prognosis of Coronary Artery Disease. *Circulation*. 2000;102.

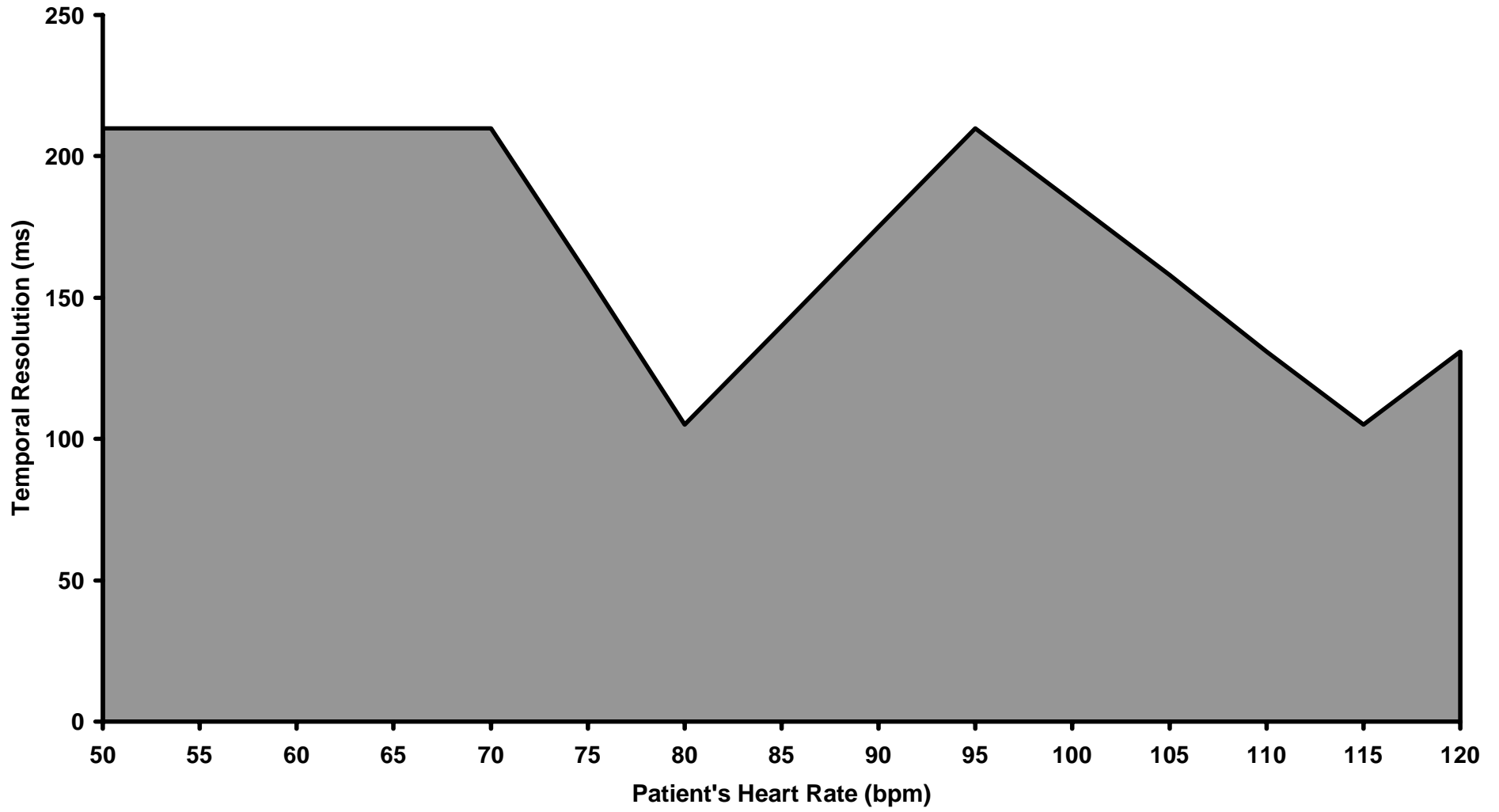


Figure 1

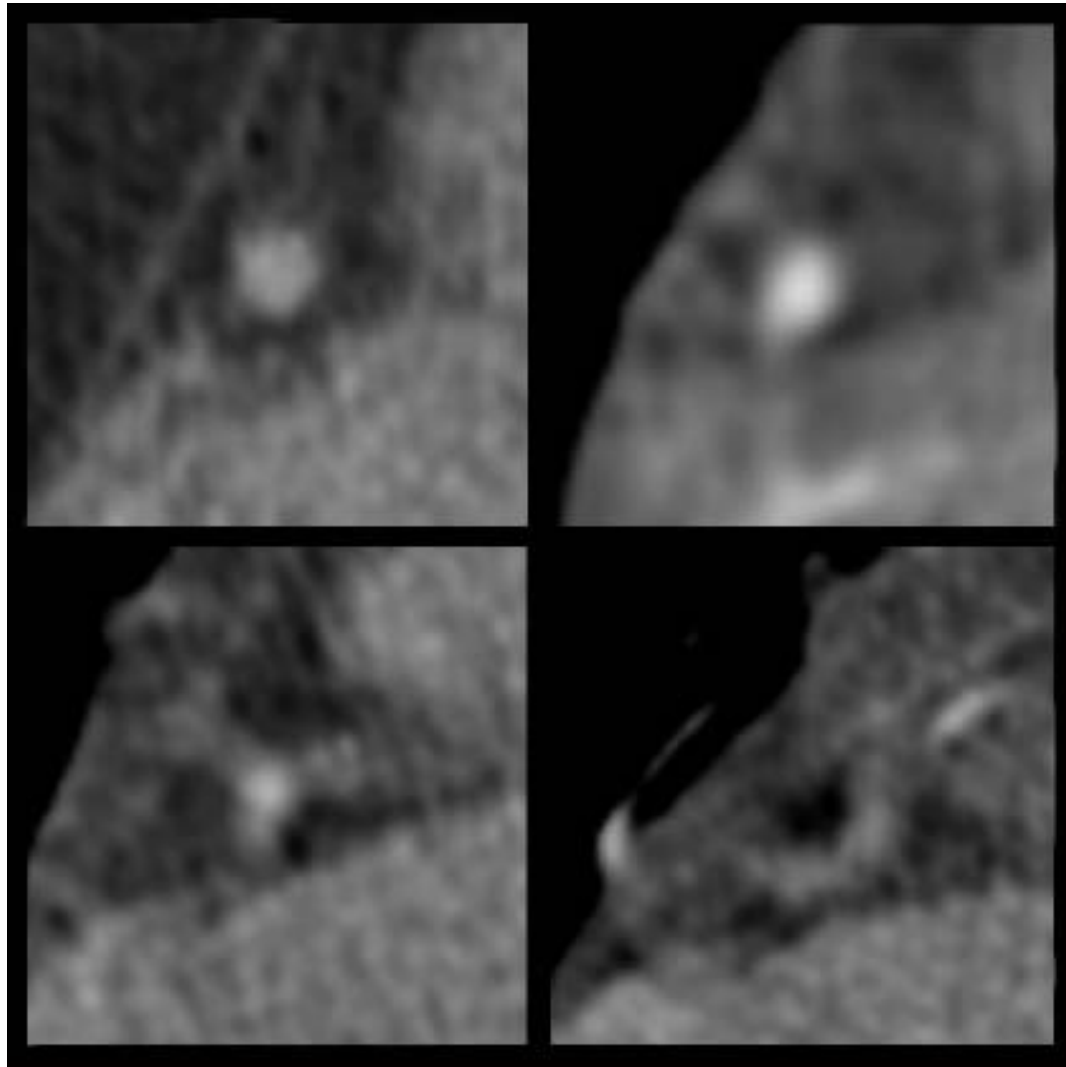


Figure 2

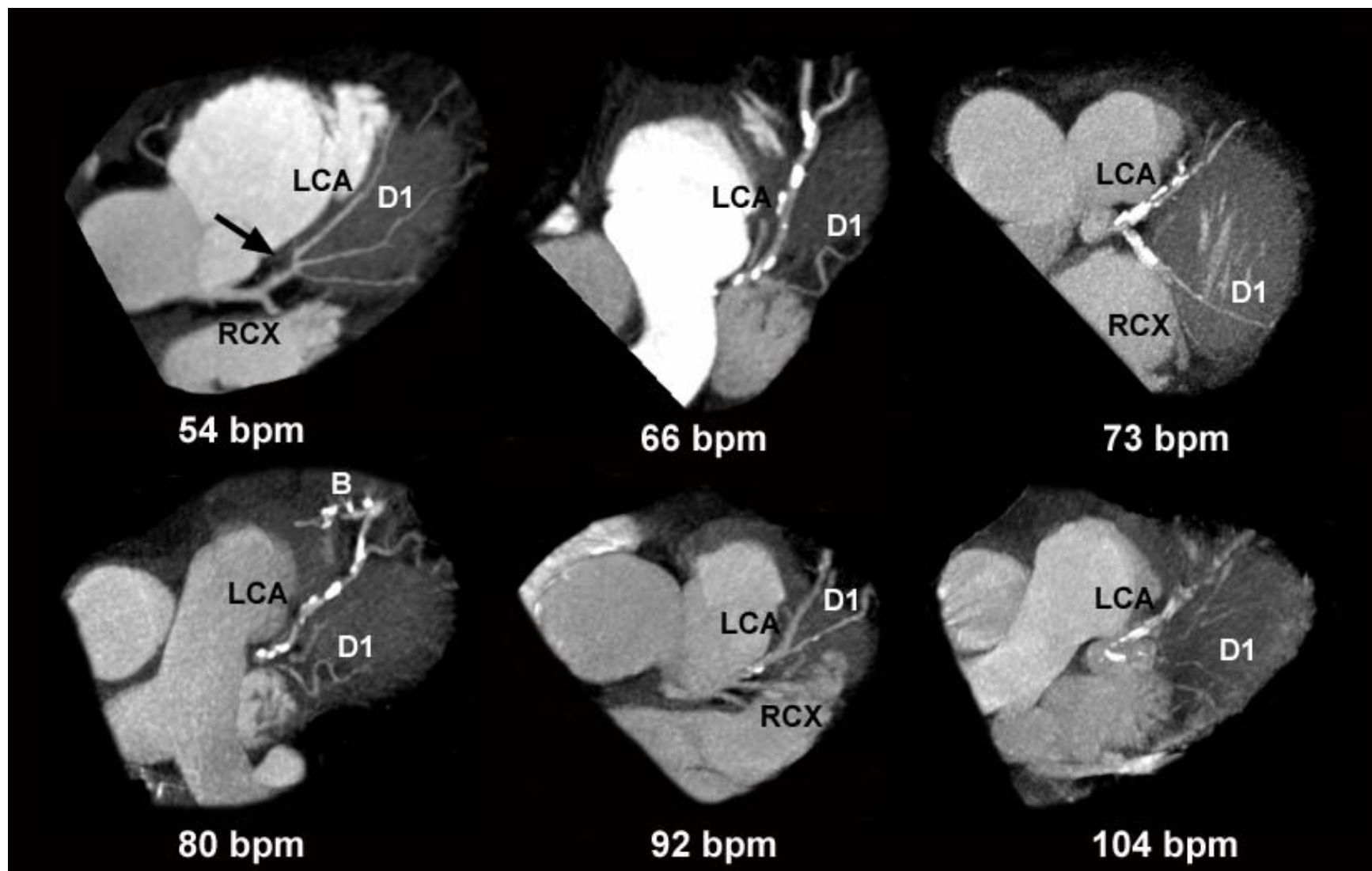


Figure 3

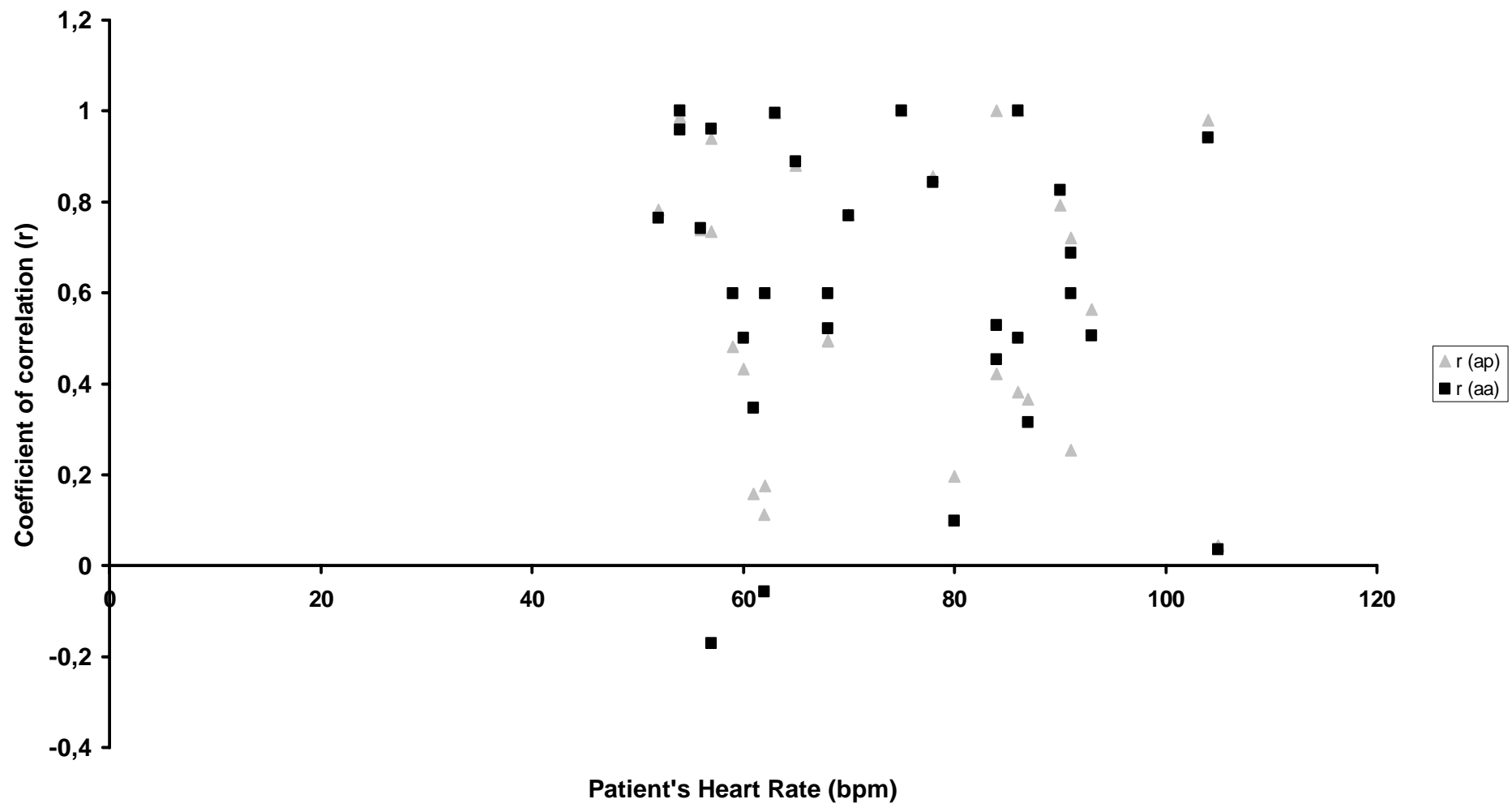


Figure 4

Figure 1 Schematic drawing, showing the actual temporal resolution of the cardiac mode of the Sensation 16 CT (Siemens, Forchheim, Germany) in dependence on the patients' heart rate. By using a multi-segment reconstruction algorithm (ACV®) highest temporal resolution (105 ms) is achieved only twice, at approximately 81 bpm and 116 bpm. For higher or lower heart rates distinct worse values are achieved, temporal resolution showing a rather linear course ranging between 210 ms ($HR \leq 72$ bpm, $HR = 94$ bpm) and 105 ms ($HR = 81$ bpm, $HR = 116$ bpm).

Figure 2 Grading (1-4) of image quality considering as example magnified views of the RCA. All images are derived from transverse scans. Excellent quality (grading 1) was attributed to vessels appearing as a clear circular/oval area surrounded by low attenuation fat tissue and showing no motion artifacts (upper row left). The same applied to calcified atherosclerotic plaques in this group. Good quality (grading 2) was attributed in the presence of discrete blurring of the vessel's or calcified plaque's margin and slight motion artifacts, seen as discrete tail or streak emitting shadow on at least one level (upper row right). Moderate image quality (grading 3) described noticeably blurred vessel- / plaque margins and distinct broader motion artifacts extending less than 5 mm from the vessels' center (lower row left). Poor image quality (grading 4) defined inadequate delineation between vessel and surrounding tissue as well as streak artifacts extending at least 5 mm from the center of the vessel (lower row right).

Figure 3 Optimal image quality achieved at different heart rates. Oblique-coronal views from the left upon the left coronary artery (LCA), the first diagonal branch (D1) and the left circumflex artery (LCX) for heart rates between 54 bpm (upper row left)

and 105 bpm (lower row right). All images were obtained by using antegrade-absolute image reconstruction. Although good image quality was achieved at heart rates of up to approximately 92 bpm, excellent image quality was achieved only at heart rates of up to approximately 66 bpm. Image 2 (upper row middle) and 4 (lower row left) originate from the same patient, the latter displaying a postoperative status. Note the left internal mammary bypass (B) attached to the LCA. The black arrow on the upper left image indicates a >50% stenosis of LCA segment 6.

Figure 4 Comparison between patient's heart rate (bpm) and total correlation coefficient of CA and MD-CTA regarding the detection and grading of coronary atherosclerosis. Displayed are the results for antegrade-proportional (grey triangles) and antegrade-absolute (black boxes) image reconstruction obtained from the 30 patient who additionally underwent coronary angiography. No correlation between the amount of heart rate and the degree of correlation can be observed.

Table 1a Optimal image quality obtained for the proximal, medial and distal RCA by using either antegrade-proportional (ap) or antegrade-absolute (aa) image reconstruction

HR	(bpm)	RCA prox			RCA med			RCA dis		
		ap (1-4)	aa (1-4)	(ap-aa) / ap (%)*	ap (1-4)	aa (1-4)	(ap-aa) / ap (%)*	ap (1-4)	aa (1-4)	(ap-aa) / ap (%)*
	46-51	1.5	1.0	33.3	1.0	1.2	(20.0)	1.4	1.4	0.0
	56-60	2.1	1.9	9.5	1.8	1.5	16.6	2.2	1.9	13.6
	61-65	2.1	2.2	(4.8)	2.3	1.9	17.4	2.2	2.0	9.1
	66-70	2.6	2.5	3.8	2.3	2.3	0.0	2.4	2.0	16.7
	71-75	2.3	2.3	0.0	2.6	2.3	11.5	2.6	2.4	7.7
	76-80	2.6	2.8	7.7	2.8	2.4	14.3	2.5	2.4	4.0
	81-85	2.8	2.2	21.4	2.5	2.0	20.0	2.6	2.2	7.7
	86-90	2.9	2.5	13.8	3.0	2.3	23.3	2.4	2.3	4.2
	91-95	2.7	2.8	(3.7)	3.0	2.6	13.3	3.0	3.0	0.0
	96-100	2.8	2.7	3.7	3.2	2.8	6.3	2.8	2.8	0.0
	101-105	3.0	3.0	0.0	3.5	3.0	14.3	3.0	2.5	16.7
	≤45 - 105	2.5	2.3	9.3	2.6	2.2	10.6	2.5	2.3	7.3

* brackets indicate negative values, thus better results for ap as compared to aa

Table 1b Optimal image quality obtained for the proximal, medial and distal LCA by using either antegrade-proportional (ap) or antegrade-absolute (aa) image reconstruction

HR	(bpm)	LCA prox			LCA med			LCA dis		
		ap (1-4)	aa (1-4)	(ap-aa)/ ap (%)*	ap (1-4)	aa (1-4)	(ap-aa) / ap (%)*	ap (1-4)	aa (1-4)	(ap-aa) / ap (%)*
46-51		1.4	1.2	14.3	1.0	1.0	0.0	1.5	1.3	13.3
56-60		1.8	1.3	27.8	1.8	1.6	(11.1)	2.3	1.6	30.4
61-65		1.9	2.2	(15.8)	2.1	1.8	14.3	2.1	1.8	14.3
66-70		2.4	1.8	(8.3)	2.3	2.0	13.0	2.2	1.9	13.6
71-75		2.3	2.2	4.3	2.4	2.2	8.3	2.6	2.4	7.7
76-80		2.2	2.0	9.1	2.4	2.7	(12.5)	2.4	2.3	4.2
81-85		2.2	2.5	(13.6)	2.7	2.3	14.8	2.4	2.2	8.3
86-90		3.0	2.2	26.7	2.7	2.0	25.9	2.6	2.4	(7.7)
91-95		2.4	2.6	(8.3)	2.6	2.5	3.8	2.7	3.0	(11.1)
96-100		3.0	2.5	16.7	3.1	2.5	19.4	3.0	2.5	16.7
101-105		3.0	2.8	6.7	2.8	2.6	7.1	3.0	2.5	16.7
≤45 - 105		2.3	2.1	17.4	2.4	2.1	9.1	2.4	2.2	8.7

* brackets indicate negative values, thus better results for ap as compared to aa

Table 1c Optimal image quality obtained for the proximal, medial and distal LCX by using either antegrade-proportional (ap) or antegrade-absolute (aa) image reconstruction

HR	(bpm)	LCX prox			LCX med			LCX dis		
		ap (1-4)	aa (1-4)	(ap-aa) / ap (%)*	ap (1-4)	aa (1-4)	(ap-aa) / ap (%)*	ap (1-4)	aa (1-4)	(ap-aa) / ap (%)*
	46-51	1.3	1.3	0	1.3	1.4	(7.6)	1.3	1.5	15.4
	56-60	1.8	1.5	16.7	1.8	1.7	5.6	2.1	1.9	9.5
	61-65	2.1	2.8	14.3	2.2	2.0	9.1	2.0	1.7	15.0
	66-70	2.8	2.0	28.6	2.6	2.2	15.4	2.4	2.0	16.7
	71-75	2.4	2.4	0.0	2.4	2.3	4.2	2.8	2.5	10.7
	76-80	2.6	2.2	15.4	2.7	2.4	11.1	3.1	2.5	19.4
	81-85	2.3	2.3	8.7	2.8	2.3	17.9	2.4	2.1	12.5
	86-90	2.9	2.5	20.7	2.5	2.2	12.0	2.8	2.4	14.3
	91-95	2.6	2.6	0.0	3.0	2.7	11.1	2.7	2.5	7.4
	96-100	3.0	2.8	6.7	2.9	2.5	13.8	3.0	2.7	10.0
	101-105	3.5	3.0	16.7	4.0	3.0	25.0	3.0	2.8	6.7
	≤45 - 105	2.5	2.2	11,6	2.6	2.2	12.1	2.5	2.2	12.5

*brackets indicate negative values, thus better results for ap as compared to aa

TABLE 2 Results of Cluster analysis, discrimination analysis and regression analysis for antegrade-proportional (ap) image reconstruction

	Cluster Analysis									Discrimination Analysis		Regression Analysis	
	Reconstruction Interval					Heart Rate				Cut-off point (bpm)	Rate of misclassification (%)	Regression equation*	p
	N° Clusters	Cluster	n	Cluster center (%)	Min. (%)	Max. (%)	Cluster center (bpm)	Min. (bpm)	Max. (bpm)				
RCA													
prox	2	ED [†]	77	59.9	40.0	75.0	60.0	45.0	81.0	67.5	10.4	58.48 + 0.02 x HR	0.22
		ES [‡]	76	26.5	10.0	35.0	82.6	62.0	131.0			30.02 - 0.04 x HR	0.92
med	2	ED	59	59.4	50.0	70.0	60.5	47.0	75.0	65.5	7.9	67.45 - 0.13 x HR	0.26
		ES	89	28.3	10	45.0	80.8	60.0	131.0			29.40 - 0.01 x HR	0.76
dis	2	ED	61	59.8	50.0	70.0	61.0	43.0	82.0	66.5	8.7	51.0 x 0.15 x HR	0.16
		ES	84	26.3	15.0	35.0	82.2	62.0	119.0			30.44 - 0.05 x HR	0.27
LCA													
prox	2	ED	76	62.2	55.0	75.0	59.0	48.0	71.0	66.5	8.7	77.89 - 0.27 x HR	10 ⁻³
		ES	66	26.3	10.0	35.0	81.0	61.0	131.0			26.86 - 0.01 x HR	0.15
med	2	ED	78	61.8	45.0	70.0	60.3	47.0	79.0	66.5	8.1	71.27 - 0.15 x HR	0.17
		ES	63	28.3	15.0	40.0	81.9	62.0	131.0			27.12 + 0.01 x HR	0.35
dis	2	ED	83	60.8	45.0	70.0	61.0	43.0	82.0	65.5	7.7	56.26 + 0.07 x HR	0.8
		ES	58	27.7	15.0	35.0	82.8	63.0	119.0			33.35 - 0.07 x HR	0.07
LCX													
prox	2	ED	76	62.2	55.0	75.0	59.0	48.0	71.0	66.5	8.7	77.88 - 0.27 x HR	10 ⁻³
		ES	66	26.3	10.0	35.0	81.0	61.0	131.0			26.86 - 0.01 x HR	0.15
med	2	ED	78	61.8	45.0	70.0	60.3	47.0	79.0	65.5	8.1	71.27 - 0.16 x HR	0.17
		ES	63	28.3	15.0	40.0	81.9	62.0	131.0			27.11 + 0.01 x HR	0.72
dis	2	ED	58	60.8	45.0	70.0	61.0	43.0	82.0	67.5	7.7	56.26 + 0.07 x HR	0.40
		ES	83	27.7	15.0	35.0	82.8	63.0	119.0			33.36 - 0.07 x HR	0.07

¹ valid only if p < 0.05. Otherwise cluster centers may serve as an approximation for optimal reconstruction intervals; [†]end-diastolic cluster; [‡]end-systolic cluster

TABLE 3 Results of Cluster analysis, discrimination analysis and regression analysis for antegrade-proportional (ap) image reconstruction

	Cluster Analysis									Discrimination Analysis		Regression Analysis	
	Reconstruction Interval					Heart Rate				Cut-off point (bpm)	Rate of misclassification (%)	Regression equation*	p
	N° Clusters	Cluster	n	Cluster center (%)	Min. (%)	Max. (%)	Cluster center (bpm)	Min. (bpm)	Max. (bpm)				
RCA													
prox	2	ED [†]	77	59.9	40.0	75.0	60.0	45.0	81.0	67.5	10.4	58.48 + 0.02 x HR	0.22
		ES [‡]	76	26.5	10.0	35.0	82.6	62.0	131.0			30.02 - 0.04 x HR	0.92
med	2	ED	59	59.4	50.0	70.0	60.5	47.0	75.0	65.5	7.9	67.45 - 0.13 x HR	0.26
		ES	89	28.3	10	45.0	80.8	60.0	131.0			29.40 - 0.01 x HR	0.76
dis	2	ED	61	59.8	50.0	70.0	61.0	43.0	82.0	66.5	8.7	51.0 x 0.15 x HR	0.16
		ES	84	26.3	15.0	35.0	82.2	62.0	119.0			30.44 - 0.05 x HR	0.27
LCA													
prox	2	ED	76	62.2	55.0	75.0	59.0	48.0	71.0	66.5	8.7	77.89 - 0.27 x HR	10 ⁻³
		ES	66	26.3	10.0	35.0	81.0	61.0	131.0			26.86 - 0.01 x HR	0.15
med	2	ED	78	61.8	45.0	70.0	60.3	47.0	79.0	66.5	8.1	71.27 - 0.15 x HR	0.17
		ES	63	28.3	15.0	40.0	81.9	62.0	131.0			27.12 + 0.01 x HR	0.35
dis	2	ED	83	60.8	45.0	70.0	61.0	43.0	82.0	65.5	7.7	56.26 + 0.07 x HR	0.8
		ES	58	27.7	15.0	35.0	82.8	63.0	119.0			33.35 - 0.07 x HR	0.07
LCX													
prox	2	ED	76	62.2	55.0	75.0	59.0	48.0	71.0	66.5	8.7	77.88 - 0.27 x HR	10 ⁻³
		ES	66	26.3	10.0	35.0	81.0	61.0	131.0			26.86 - 0.01 x HR	0.15
med	2	ED	78	61.8	45.0	70.0	60.3	47.0	79.0	65.5	8.1	71.27 - 0.16 x HR	0.17
		ES	63	28.3	15.0	40.0	81.9	62.0	131.0			27.11 + 0.01 x HR	0.72
dis	2	ED	58	60.8	45.0	70.0	61.0	43.0	82.0	67.5	7.7	56.26 + 0.07 x HR	0.40
		ES	83	27.7	15.0	35.0	82.8	63.0	119.0			33.36 - 0.07 x HR	0.07

¹ valid only if p < 0.05. Otherwise cluster centers may serve as an approximation for optimal reconstruction intervals; [†]end-diastolic cluster; [‡]end-systolic cluster

Table 4 Segmental and total correlation coefficients regarding detection and grading of coronary atherosclerosis. Comparison between antegrade-proportional and antegrade-absolute image reconstruction technique.

Segment	Antegrade-proportional		Antegrade-absolut	
	r	p	r	p
1	0.55	0.002	0.57	<0.001
2	0.45	< 0.020	0.51	0.003
3	0.38	0.382	0.44	0.014
4	0.49	0.493	0.61	<0.001
5	0.56	< 0.002	0.60	<0.001
6	0.78	0.787	0.79	<0.001
7	0.39	0.399	0.41	0.020
8	0.72	< 0.002	0.74	<0.001
9	0.52	0.520	0.71	<0.001
10	0.11	> 0.200	0.21	0.256
11	0.68	0.682	0.78	<0.001
12	0.05	0.050	0.55	0.0013
13	0.40	< 0.050	0.59	<0.001
14	0.26	< 0.200	0.35	0.057
15	0.00	> 0.200	0.18	0.325
Total	0.52	<0.01	0.57	<0.01